Defective Double-Cubane, Tetranuclear Manganese(II) and Cobalt(II) Complexes with Simultaneous $\mu_{1,1}$-Azido and μ-O Bridges

Giannis S. Papaefstathiou,[a][‡] Albert Escuer,[b] Catherine P. Raptopoulou,[c] Aris Terzis,*[c] Spyros P. Perlepes,*[a] and Ramon Vicente*[b]

Keywords: Azides / Cobalt / Di-2-pyridyl ketone / Magnetic properties / Manganese

The reactions of $M(O_2CCH_3)_2{\cdot}4H_2O$ (M= Mn, Co) with di-2-pyridyl ketone, $(py)_2CO$, and NaN_3 in CH_3OH or CH_3OH/H_2O allow isolation of the tetranuclear compounds $[Mn_4(\mu_{1,1}\text{-}N_3)_2(N_3)_2\{(py)_2C(OH)O\}_2\{(py)_2C(OCH_3)O\}_2]$ (**1**) and $[Co_4(\mu_{1,1}\text{-}N_3)_2(N_3)_2\{(py)_2C(OH)O\}_2\{(py)_2C(OCH_3)O\}_2]{\cdot}2H_2O$ (**2**). X-ray diffraction analysis reveals defective double-cubane tetrameric entities in which the Mn^{II} or Co^{II} atoms are linked by $\mu_{1,1}\text{-}N_3$ bridges and two kinds of O-bridges. The molar magnetic susceptibility measurements of **1** and **2** in the 2–300 K range indicate weak antiferromagnetic coupling for **1** and clear bulk ferromagnetic coupling for **2**.

Introduction

There is currently a great deal of interest in the synthesis of polynuclear metal complexes exhibiting ground electronic states with a large number of unpaired electrons, since it has been discovered that a fairly large ground-state *S* value is one of the necessary requirements for molecules to be able to exhibit the behaviour of a single-molecule magnet.[1−3] The high-spin ground state results from either ferromagnetic (or ferrimagnetic) exchange interactions between the metal ions in the molecule, or topologically frustrated antiferromagnetic interactions.[4] In the known polynuclear SMM's, magnetic exchange interactions are propagated by bridging OH^-, OR^-, O^{2-}, or RCO_2^- ligands, or a combination of two or more of these groups. These interactions often lead to antiferromagnetic coupling and, thus, it is necessary to arrange the metal ions and bridging ligands in an appropriate manner so that they can give a high-spin ground state for the system. An alternative attractive approach would be the replacement of one or more of the above-mentioned bridging ligands with other groups that are more prone to ferromagnetic coupling.

One of the most well-known ferromagnetic couplers is the azido ligand when it bridges metal ions in the 1,1-fashion. Azides usually bridge through the two terminal nitrogen atoms (μ-1,3-azido) or through only one of the terminal nitrogen atoms (μ-1,1-azido) (Scheme 1). In the latter case, the coupling between the bridged paramagnetic metal ions is ferromagnetic for a wide range of M−N−M angles.[5]

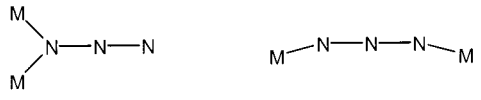

$\mu_{1,1}\text{-}N_3^-$ $\mu_{1,3}\text{-}N_3^-$

Scheme 1

The structural and electronic versatility of the azido ligand has prompted researchers to investigate its coordination chemistry in order to probe deeper into the exchange interactions of azido-bridged complexes and to correlate magnetic behaviour with molecular structure. For example, the work performed on azido-bridged polynuclear manganese(II) complexes has become a fast growing research field, not only due to the large variety of topologies that these compounds adopt, but also because of the interesting magnetic properties that arise from these systems.[6−25] In some of these compounds, the two different bridging coordination modes of the azido ligand (Scheme 1) can be found simultaneously in the same molecule, leading to materials which alternate the ferro- and antiferromagnetic superexchange pathways.

On the other hand, employment of di-2-pyridyl ketone, $(py)_2CO$ (**I**, Scheme 2), as a templating ligand for the synthesis of polynuclear complexes, has resulted, amongst others, in the construction of tetra-,[26−33] hepta-,[34] octa-,[35,36] nona-[32] and dodecanuclear[34] metal cages. The ability of $(py)_2CO$ to undergo metal-mediated nucleophilic addition of small molecules, such as water or alcohols (ROH), to the carbonyl group results in the formation of the hydrate **II** or the hemiacetal **III** (Scheme 2). The structural diversity of the resultant species stems from the ability of the singly and doubly deprotonated anions of the *gem*-diol form **II** to adopt a variety of coordination modes, and sometimes two different modes may also occur in the same complex. The monoanions of **II** and **III** usually bridge three and two metal ions, respectively (Scheme 3), giving rise to high nuclearity metal cages, while the dianion of **II** can bridge as many as five metal ions, resulting in higher nuclearity metal complexes. Since the degree of deprotonation of the *gem*-diol $(py)_2C(OH)_2$ (**II**) has been well established,

[a] Department of Chemistry, University of Patras, 265 00 Patras, Greece
[b] Departament de Química Inorgànica, Universitat de Barcelona, Diagonal 647, 08028 Barcelona, Spain
[c] Institute of Materials Science, NCSR "Demokritos", 153 10 Aghia Paraskevi Attikis, Greece
[‡] ERASMUS student in Barcelona

  1434−1948/01/0606−1567 $ 17.50+.50/0

the nuclearity of the resultant species can be considered more or less as "controlled".

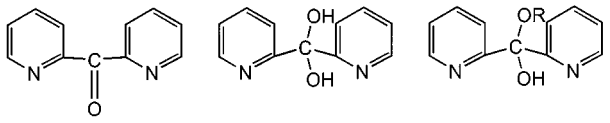

$(py)_2CO$, **I** $(py)_2C(OH)_2$, **II** $(py)_2C(OR)OH$, **III**

Scheme 2

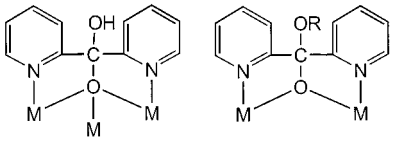

$\eta^1:\eta^3:\eta^1:\mu_3$ $\eta^1:\eta^2:\eta^1:\mu_2$

Scheme 3

The magnetic properties of the metal cages based on the anions of **II** range from noninteracting[28] to antiferromagnetic[29,30,32,34–36] and ferromagnetic-coupled[26,27,31,32] systems. This variety of magnetic properties is a consequence of the metal topology that the cages adopt, which is influenced not only by the coordination mode of the $(py)_2CO$-based anions but also by the other ligands present in the structure. Therefore, an interesting possibility is to combine the azido and $(py)_2CO$-based anionic ligands in the same compound. We report here the synthesis and magneto-structural characterisation of the tetranuclear compound $[Mn_4(\mu_{1,1}\text{-}N_3)_2(N_3)_2\{(py)_2C(OH)O\}_2\{(py)_2C(OCH_3)O\}_2]$ (**1**). In this compound the azido bridging coordination mode is end-on and should furnish a ferromagnetic superexchange pathway. We also report the synthesis and magneto-structural characterisation of the analogous cobalt(II) compound $[Co_4(\mu_{1,1}\text{-}N_3)_2(N_3)_2\{(py)_2C(OH)O\}_2\{(py)_2C(OCH_3)O\}_2]\cdot 2H_2O$ (**2**). The interest in this new compound, apart from the above considerations, is found in the fact that polynuclear Co^{II} compounds with azido bridging ligands are rare.[37–44] Previously, only two mixed azido-$(py)_2CO$ complexes with Ni^{II} as the metal ion have been published.[26,27]

Results and Discussion

Synthesis

The preparation of compounds **1** and **2** can be achieved by the reaction of $M(O_2CH_3)_2 4H_2O$ with $(py)_2CO$ and NaN_3 in CH_3OH (**1**) or CH_3OH/H_2O (**2**) at room temperature. The preparation of both complexes can be summarised by Equation (1).

The metal(II)-mediated solvolysis of $(py)_2CO$ to give the monoanions of the hydrate **II** and the hemiacetal **III** (Scheme 2) involves a nucleophilic attack of ROH molecules (R = Me or H) on the carbonyl group. In such reactions it might not be necessary for the carbonyl atom to be coordinated to the metal centre; the induced polarisation from the pyridyl nitrogen atoms might be sufficient.[45] There are few examples in which the ketone group of $(py)_2CO$ is attacked by alcohols or water in the presence of metal ions, but the presence of the monoanions of both the hydrate and the hemiacetal in the same complex is rare, with the $[Ni_4(\mu_{1,1}\text{-}N_3)_2(N_3)_2\{(py)_2C(OH)O\}_2\{(py)_2C(OCH_3)O\}_2]$[26] complex being the only example until now.

IR Spectra

Complexes **1** and **2** exhibit identical IR spectra and, thus, only the IR spectrum of **1** is discussed. This complex exhibits an intense band centred at 2061 cm^{-1}, assigned to the asymmetric stretching mode of the azide. This band is split (2074 and 2048 cm^{-1}) due to the presence of two coordination modes of the azide in the molecular structure of **1**. The spectrum does not exhibit a band in the region expected for $\nu(C{=}O)$ absorption [1684 cm^{-1} for the free $(py)_2CO$]. The nearest band is at 1600 cm^{-1} and is assigned as a pyridine stretching mode raised from 1582 cm^{-1} on coordination, as observed previously,[30] on complex formation involving the solvolysis of $(py)_2CO$. Additionally, the spectrum reveals the bands corresponding to the skeleton vibrations of the coordinated $(py)_2CO$ which appear at slightly shifted frequencies relative to the free ligand. Thus, bands for coordinated $\{(py)_2C(OR)O\}^-$ [free $(py)_2CO$] are: 1570 [1578/1544] and 1114 [998] cm^{-1} attributed to the pyridyl ring stretching, 774/754 [753/742] for the pyridyl ring C–H out-of-plane bending, and 680 [662] due to the pyridyl ring in-plane vibration.

X-ray Crystal Structures

$[Mn_4(\mu_{1,1}\text{-}N_3)_2(N_3)_2\{(py)_2C(OH)O\}_2\{(py)_2C(OCH_3)O\}_2]$ (1)

A labelled plot of the structure of the tetranuclear compound $[Mn_4(\mu_{1,1}\text{-}N_3)_2(N_3)_2\{(py)_2C(OH)O\}_2\{(py)_2C(OCH_3)\text{-}O\}_2]\cdot 2H_2O$ (**1**) is shown in Figure 1. Selected distances and angles are listed in Table 1. The structure consists of centrosymmetric tetranuclear molecules. The four Mn^{II} atoms are located at four corners of a defective double

$$4M(O_2CCH_3)_2\cdot 4H_2O + 4NaN_3 + 4(py)_2CO + 2CH_3OH + nH_2O \xrightarrow[20\,^\circ C]{S} [M_4(\mu_{1,1}\text{-}N_3)_2(N_3)_2\{(py)_2C(OH)O\}_2\{(py)_2C(OCH_3)O\}_2]\cdot nH_2O + 4CH_3CO_2H + 4CH_3CO_2Na + 14H_2O \quad (1)$$

1: M = Mn^{II}, S = CH_3OH

2: M = Co^{II}, n = 2, S = CH_3OH/H_2O

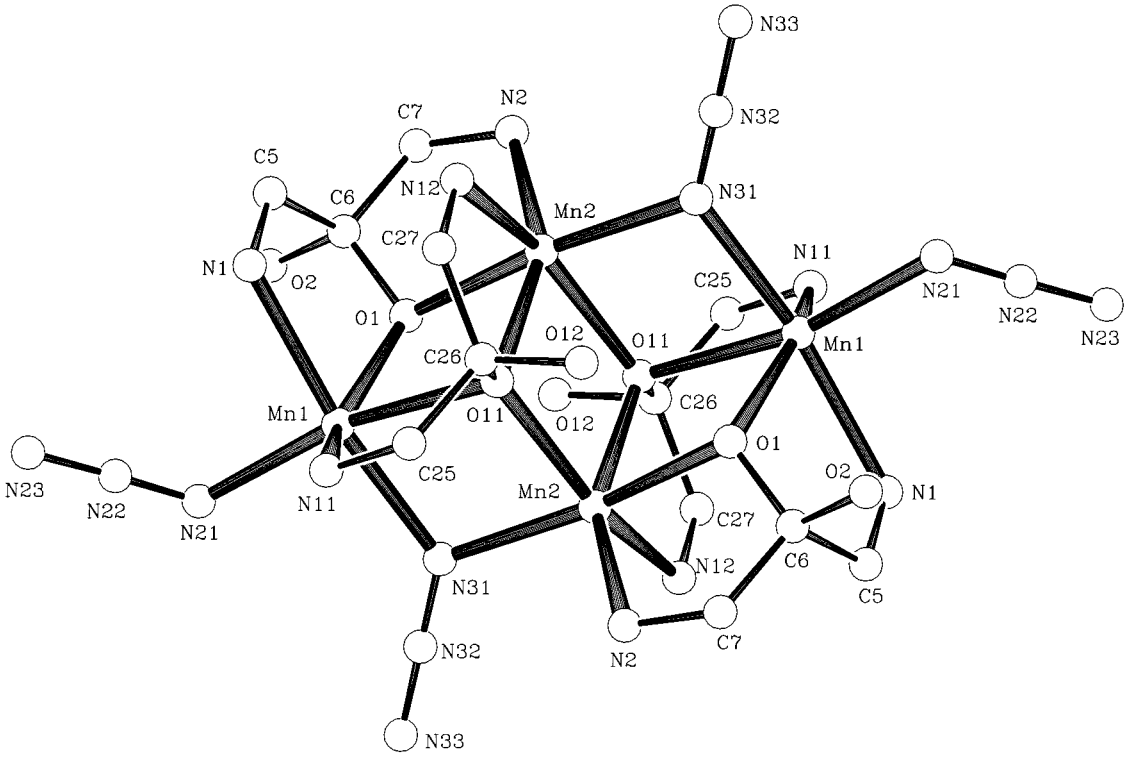

Figure 1. Labelled plot of $[Mn_4(\mu_{1,1}\text{-}N_3)_2(N_3)_2\{(py)_2C(OH)O\}_2\{(py)_2C(OCH_3)\text{-}O\}_2]\cdot 2H_2O$ (**1**); the structure and numbering of the atoms is the same for compound **2**, replacing Mn(1) and Mn(2) with Co(1) and Co(2), respectively

Table 1. Selected distances (Å) and angles (°) for $[Mn_4(\mu_{1,1}\text{-}N_3)_2(N_3)_2\{(py)_2C(OH)O\}_2\{(py)_2C(OCH_3)O\}_2]$ (**1**)[a]

Mn(1)···Mn(2)	3.370(1)	Mn(1)···Mn(2)#1	3.395(3)
Mn(1)···Mn(1)#1	5.892(1)	Mn(2)···Mn(2)#1	3.322(3)
Mn(1)−N(21)	2.111(5)	Mn(1)−O(1)	2.155(3)
Mn(1)−N(31)	2.210(5)	Mn(1)−N(11)	2.287(5)
Mn(1)−N(1)	2.305(5)	Mn(1)−O(11)	2.305(3)
Mn(2)−O(11)	2.137(3)	Mn(2)−N(31)#1	2.167(4)
Mn(2)−O(11)#1	2.186(3)	Mn(2)−N(2)	2.218(4)
Mn(2)−O(1)	2.242(3)	Mn(2)−N(12)	2.279(4)
O(1)−C(6)	1.378(6)	O(11)−C(26)	1.399(6)
N(31)−N(32)	1.195(6)	N(21)−N(22)	1.170(8)
N(22)−N(23)	1.167(9)	N(32)−N(33)	1.152(8)
N(21)−Mn(1)−O(1)	114.7(2)	N(21)−Mn(1)−N(31)	94.0(2)
O(1)−Mn(1)−N(31)	97.2(2)	N(21)−Mn(1)−N(11)	96.9(2)
O(1)−Mn(1)−N(11)	145.8(2)	N(31)−Mn(1)−N(11)	93.2(2)
N(21)−Mn(1)−N(1)	90.8(2)	O(1)−Mn(1)−N(1)	71.7(1)
N(31)−Mn(1)−N(1)	168.8(2)	N(11)−Mn(1)−N(1)	96.2(2)
N(21)−Mn(1)−O(11)	165.3(2)	O(1)−Mn(1)−O(11)	78.7(1)
N(31)−Mn(1)−O(11)	77.5(1)	N(11)−Mn(1)−O(11)	71.8(1)
N(1)−Mn(1)−O(11)	99.7(1)	O(11)−Mn(2)−N(31)#1	107.5(2)
O(11)−Mn(2)−O(11)#1	79.5(1)	N(31)#1−Mn(2)−O(11)#1	81.0(1)
O(11)−Mn(2)−N(2)	152.6(1)	N(31)#1−Mn(2)−N(2)	99.7(2)
O(11)#1−Mn(2)−N(2)	107.7(1)	O(11)−Mn(2)−O(1)	80.5(1)
N(31)#1−Mn(2)−O(1)	164.4(2)	O(11)#1−Mn(2)−O(1)	87.6(1)
N(2)−Mn(2)−O(1)	73.6(1)	O(11)−Mn(2)−N(12)	73.4(1)
N(31)#1−Mn(2)−N(12)	92.5(2)	O(11)#1−Mn(2)−N(12)	148.9(1)
N(2)−Mn(2)−N(12)	103.3(2)	O(1)−Mn(2)−N(12)	102.6(1)
Mn(1)−O(1)−Mn(2)	100.0(1)	Mn(2)−O(11)−Mn(2)#1	100.4(1)
Mn(2)−O(11)−Mn(1)	98.6(1)	Mn(2)#1−O(11)−Mn(1)	98.1(1)
N(22)−N(21)−Mn(1)	125.1(5)	N(32)−N(31)−Mn(2)#1	125.0(4)
N(32)−N(31)−Mn(1)	131.8(4)	Mn(2)#1−N(31)−Mn(1)	101.7(2)
N(23)−N(22)−N(21)	179.4(10)	N(33)−N(32)−N(31)	179.0(8)

[a] Symmetry transformations used to generate equivalent atoms #1: $-x, -y, -z + 1$.

Table 2. Selected distances (Å) and angles (°) for $[Co_4(\mu_{1,1}\text{-}N_3)_2(N_3)_2\{(py)_2C(OH)O\}_2\{(py)_2C(OCH_3)O\}_2]\cdot 2H_2O$ (**2**)[a]

Co(1)···Co(2)	3.184(1)	Co(1)···Co(2)#1	3.286(1)
Co(1)···Co(1)#1	5.640(1)	Co(2)···Co(2)#1	3.172(1)
Co(1)−O(1)	2.063(2)	Co(1)−N(21)	2.083(3)
Co(1)−N(31)	2.099(3)	Co(1)−N(11)	2.115(3)
Co(1)−N(1)	2.170(3)	Co(1)−O(11)	2.227(2)
Co(2)−O(11)	2.030(2)	Co(2)−N(31)#1	2.058(3)
Co(2)−N(2)	2.089(3)	Co(2)−N(12)	2.151(3)
Co(2)−O(1)	2.151(2)	Co(2)−O(11)#1	2.165(2)
O(1)−C(6)	1.378(3)	O(11)−C(26)	1.379(3)
N(31)−N(32)	1.193(4)	N(21)−N(22)	1.141(5)
C(6)−O(2)	1.424(4)	N(22)−N(23)	1.139(6)
N(32)−N(33)	1.141(4)		
O(1)−Co(1)−N(21)	110.8(1)	O(1)−Co(1)−N(31)	94.4(1)
N(21)−Co(1)−N(31)	91.1(1)	O(1)−Co(1)−N(11)	148.2(1)
N(21)−Co(1)−N(11)	97.8(1)	N(31)−Co(1)−N(11)	98.8(1)
O(1)−Co(1)−N(1)	75.4(1)	N(21)−Co(1)−N(1)	89.8(1)
N(31)−Co(1)−N(1)	169.3(1)	N(11)−Co(1)−N(1)	91.6(1)
O(1)−Co(1)−O(11)	80.4(1)	N(21)−Co(1)−O(11)	164.9(1)
N(31)−Co(1)−O(11)	77.6(1)	N(11)−Co(1)−O(11)	74.4(1)
N(1)−Co(1)−O(11)	103.1(1)	O(11)−Co(2)−N(31)#1	103.8(1)
O(11)−Co(2)−N(2)	154.9(1)	N(31)#1−Co(2)−N(2)	99.8(1)
O(11)−Co(2)−N(12)	77.6(1)	N(31)#1−Co(2)−N(12)	91.1(1)
N(2)−Co(2)−N(12)	93.7(1)	O(11)−Co(2)−O(1)	83.0(1)
N(31)#1−Co(2)−O(1)	164.4(1)	N(2)−Co(2)−O(1)	76.3(1)
N(12)−Co(2)−O(1)	104.2(1)	O(11)−Co(2)−O(11)#1	81.8(1)
N(31)#1−Co(2)−O(11)#1	79.9(1)	N(2)−Co(2)−O(11)#1	110.9(1)
N(12)−Co(2)−O(11)#1	154.8(1)	O(1)−Co(2)−O(11)#1	87.3(1)
Co(1)−O(1)−Co(2)	98.1(1)	Co(2)−O(11)−Co(2)#1	98.2(1)
Co(2)−O(11)−Co(1)	96.7(1)	Co(2)#1−O(11)−Co(1)	96.8(1)
N(22)−N(21)−Co(1)	131.7(3)	N(32)−N(31)−Co(2)#1	127.4(2)
N(32)−N(31)−Co(1)	125.5(2)	Co(2)#1−N(31)−Co(1)	104.5(1)
N(23)−N(22)−N(21)	178.2(7)	N(33)−N(32)−N(31)	178.9(4)

[a] Symmetry transformations used to generate equivalent atoms #1: $-x+1, -y, -z+2$.

cubane (two cubanes sharing one face and each missing one vertex) and bridged by means of two end-on azido ligands and O atoms from the $(py)_2C(OH)O^-$ and $(py)_2C(OCH_3)O^-$ anions (Scheme 3). Peripheral ligation is provided by the nitrogen atoms of the two terminal azido ligands and the eight 2-pyridyl rings. The O(11) atoms of the $(py)_2C(OH)O^-$ ligands are triply bridging with distances to the Mn^{II} atoms in the range 2.137(3)−2.305(3) Å. The Mn(1)−O(11)−Mn(2) angles are 98.1(1)° and 98.6(1)°. The O(1) atoms of the $(py)_2C(OCH_3)O^-$ ligands are doubly bridging with distances of 2.155(3) and 2.242(3) Å to Mn(1) and Mn(2), respectively. The Mn(1)−O(1)−Mn(2) angle is 100.0(1)°. One O atom of each $(py)_2C(OH)O^-$ and $(py)_2C(OCH_3)O^-$ ligands remains protonated and unbound to the metal atoms. Mn(1) and Mn(2) are also bridged by the N(31) atom of the $\mu_{1,1}$-azido ligand. The Mn(1)−N(31) and Mn(2)−N(31) distances are 2.210(5) and 2.167(4) Å, respectively. The Mn(1)−N(31)−Mn(2) angle is 101.7(2)°. The Mn(1) octahedral coordination is completed by the N(11) atom of the $(py)_2C(OH)O^-$ ligand, the N(1) atom of the $(py)_2C(OCH_3)O^-$ ligand and the N(21) atom of the terminal azido ligand. The Mn(2) octahedral coordination is completed by the N(2) and the N(12) atoms of the $(py)_2C(OCH_3)O^-$ and $(py)_2C(OH)O^-$ ligands, respectively.

$Co_4(\mu_{1,1}\text{-}N_3)_2(N_3)_2\{(py)_2C(OH)O\}_2\{(py)_2C(OCH_3)O\}_2]\cdot 2H_2O$ (2)

Selected distances and angles are presented in Table 2. The structure of **2** is very similar to the structure of **1**. As expected, distances and angles are slightly different with respect to the analogous parameters in **1**: bond lengths are shorter in **2** and bond angles in the bridging region are ±3°, for details see Table 2.

Magnetic Properties

The $\chi_M T$ vs. T plot of **1** in the 300−2 K range is shown in Figure 2. $\chi_M T$ has a practically constant value of 17.1 cm^3 K mol^{-1} in the 300−115 K range and then decreases to 14.3 cm^3 K mol^{-1} at 2 K. χ_M increases on cooling and does not have any maximum in the studied temperature range. The overall behaviour of **1** indicates a dominant weak antiferromagnetic coupling. The magnetic data of **1**, according to its structure (Scheme 4), should be analysed by an analytical expression based on the Hamiltonian in Equation (2)

$$H = -J_1(S_1S_2 + S_3S_4) - J_2(S_2S_3 + S_4S_1) - J_3(S_2S_4) - J_4(S_1S_3) \quad (2)$$

for local spin values $S = 5/2$. The number of the spins follows the numbering of the atoms in Scheme 4 (J_4 correlates atoms 1 and 3).

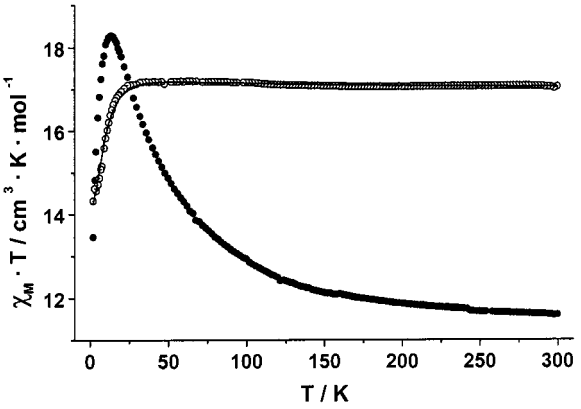

Figure 2. $\chi_M T$ plot versus T for compounds **1** (dot centred circles) and **2** (filled circles); solid lines correspond to the best fit obtained for **1**

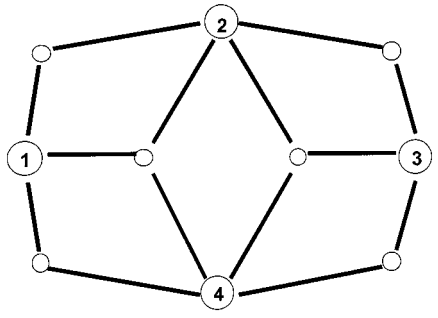

Scheme 4

Although the analytical expression with four different J values does not exist, the eigen values of the spin states can be calculated by means of the full-matrix diagonalisation of Equation (2), by using the CLUMAG program.[47] The best-fit parameters obtained were $J_1 = -1.56$ cm^{-1}, $J_2 = 0.53$ cm^{-1}, $J_3 = -1.49$ cm^{-1}, $J_4 = -0.01$ cm^{-1}, $g = 1.98$, $R = 2.1 \times 10^{-5}$.

The molar magnetisation data at 2 K in the 0−5 T range are shown in Figure 3. On increasing the field, the magnetisation value increases slowly with reference to the expected value for four isolated Mn^{II} atoms with $g = 2.0$, and the final value of 14.91 is far from the expected value of 20, which is in agreement with a dominant antiferromagnetic coupling. The coupling between Mn(2) and Mn(1) through the $\mu_{1,1}$-azido ligand with a Mn−N−Mn angle of 101.7(2)° should be ferromagnetic,[5] but for complexes containing the $\{Mn_2(\mu_2\text{-OR})_2\}^{2+}$ core and an Mn−O−Mn angle in the range of 80−110°, the coupling should be antiferromagnetic,[48] as is the case in **1**. For this reason the superexchange pathway through simultaneous $\mu_{1,1}$-azido and μ-O bridges is indeterminate in sign. From Equation (2), J_1 and J_2 are indistinguishable by symmetry; the values of $J_1 = -1.56$ cm^{-1} and $J_2 = 0.53$ cm^{-1} may be reasonably assigned, by sign, to the $(\mu_2\text{-OR})_2$ and {(μ-OR)($\mu_{1,1}$-Azido)} superexchange pathways, respectively. The value of $J_3 = -1.49$ cm^{-1} is in accordance with a superexchange pathway only through the μ-O bridges. The negligible value of J_4 is, as expected, due to the large distance between the 1 and 3 spin carriers. The EPR spectrum of **1** recorded on a powdered sample at room temperature shows an isotropic signal centred at $g = 2.02$ with a peak-to-peak line width of 1340 G. This signal is temperature dependent and the spectrum at 4 K shows a complicated pattern of signals.

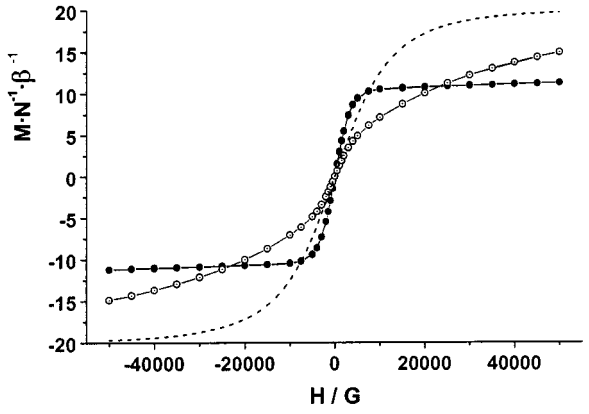

Figure 3. Molar magnetisation isotherms at 2 K for compounds **1** (dot centred circles) and **2** (filled circles); the dashed line corresponds to the generated Brillouin behaviour for four isolated Mn^{II} ions

The plot of $\chi_M T$ vs. T for **2** in the 300−2 K range is also shown in Figure 2 (filled circles). $\chi_M T$ increases quickly on cooling from 11.60 cm^3 K mol^{-1} at 300 K to a maximum of 18.3 cm^3 K mol^{-1} at 13 K, after which it decreases to 13.4 cm^3 K mol^{-1} at 2 K. χ_M increases on cooling and does not have any maximum in the temperature range studied. The overall behaviour of **2** corresponds to a ferromagnetically coupled system. The strong ferromagnetic interaction in **2** is confirmed by the molar magnetisation measurement at 2 K, which shows a quick increase in M by increasing the external field, arriving at a final value of 11.26 (Figure 3). This strong coupling between Co(2) and Co(1) permits us to assume that the interactions through the $\mu_{1,1}$-azido and the μ-OR$^-$ bridge with a Co−O−Co angle of 96.8(1)° are both ferromagnetic, indicating a magnetic behaviour close to the related Ni^{II} derivatives previously reported.[26,27] Analysis of the coupling constants for a high-spin rhombic cobalt(II) tetramer is not possible by means of an effective Hamiltonian based on four $S = 3/2$ spins, due to the large anisotropy of this ion. At low temperature the local spin of the Co^{II} is closer to 1/2, and hence the low-temperature data are better defined as an $S_T = 2$ system with a large g_{eff} value.

The above description is in agreement with the EPR spectrum of **2** recorded on a powdered sample at 4 K (Figure 4), which shows only one absorption at very low field. For an axial integer $S = 2$ spin system, the zero-field interaction (D parameter) splits the m_s levels into two doublets $m_s = |\pm 2>$ and $|\pm 1>$ and one $m_s = |0>$ state. Transitions be-

tween these Kramer doublets are not possible due to the large D value expected for the cobalt(II) ion. For a rhombic distortion, the E parameter splits the $m_s = |\pm 2>$ and $|\pm 1>$ Kramer doublets giving a Δ_2 and Δ_1 gap at zero field. The Δ_1 increase is strongly dependent on E and is usually much greater than the $g\beta H$ energy of an X-band measurement. In contrast, the Δ_2 increase is a function of E^2/D and the ± 2 transition usually lies in the low-field region of the spectra.[49] The expected spectra for an $S = 2$ system then consist of only one signal at very low field, which is in agreement with the experimental spectrum of **2**, and the above assumption to avoid treatment of this system as a simple tetramer of 3/2 spins is correct. This type of EPR spectra is similar to those of manganese(III) and iron(IV) spectra reported in the literature.[50,51]

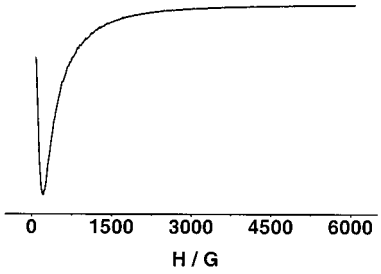

Figure 4. X-band EPR spectrum of a powdered sample of compound **2**, showing the ± 2 transition at low field corresponding to the $S = 2$ anisotropic ground state

Experimental Section

Physical Methods: Magnetic susceptibility measurements were carried out for polycrystalline samples of **1** and **2** with a SQUID susceptometer working in the range 2−300 K under magnetic fields of approximately 0.1 T. Diamagnetic corrections were estimated from Pascal Tables. The infrared spectra (4000−400 cm^{-1}) were recorded from KBr pellets on a Nicolet 520 FTIR spectrometer. EPR spectra were recorded on a Bruker ES200 spectrometer at X-band frequency.

Preparation of $[Mn_4(\mu_{1,1}\text{-}N_3)_2(N_3)_2\{(py)_2C(OH)O\}_2\{(py)_2C(OCH_3)O\}_2]$ (1): Solid $Mn(O_2CCH_3)_2{\cdot}4H_2O$ (0.15 g, 0.61 mmol) was dissolved with stirring in a solution of $(py)_2CO$ (0.22 g, 1.19 mmol) and NaN_3 (0.08 g, 1.23 mmol) in CH_3OH (20 cm^3). The pale brown-yellow solution was allowed to slowly concentrate by evaporation at room temperature for 24 h. The resultant orange well-formed crystals were collected by filtration, washed with small amounts of CH_3OH (5 cm^3) and Et_2O (2 × 5 cm^3), and dried in vacuo. Yield: 95 mg, 50%. − $C_{46}H_{40}Mn_4N_{20}O_8$ (1220.7): calcd. C 45.26, H 3.30, N 22.95; found C 45.12, H 3.28, N 22.97. − Selected IR data (KBr pellet): $\tilde{\nu}$ = 3074 (w), 2964 (w), 2074 (vs), 2048 (vs), 1600 (s), 1570 (m), 1470 (m), 1438 (s), 1334 (m), 1060 (s), 1014 (m), 776 (m), 754 (m), 680 (m) cm^{-1}. Complex **1** can also be isolated by employing $Mn(O_2CCH_3)_2 4H_2O/(py)_2CO/NaN_3$ molar ratios of 1:1:1, 1:3:3, 1:2:4 and 1:4:4.

Preparation of $[Co_4(\mu_{1,1}\text{-}N_3)_2(N_3)_2\{(py)_2C(OH)O\}_2\{(py)_2C(OCH_3)O\}_2]{\cdot}2H_2O$ (2): A solution of NaN_3 (0.04 g, 0.61 mmol) in H_2O (5 cm^3) was added to a stirred solution of $Co(O_2CCH_3)_2{\cdot}4H_2O$ (0.15 g, 0.61 mmol) and $(py)_2CO$ (0.11 g, 0.60 mmol) in CH_3OH (20 cm^3) at ambient temperature. Crystallisation of a pink solid began after ca. 20 min. When precipitation was judged to be complete, the pink microcrystalline solid was collected by filtration, washed with small amounts of CH_3OH (5 cm^3) and Et_2O (2 × 5 cm^3), and dried in vacuo. Yield: 140 mg, 75%. − $C_{46}H_{44}Co_4N_{20}O_{10}$ (1272.7): calcd. C 43.41, H 3.48, N 22.01; found C 43.60, H 3.32, N 22.38. − Selected IR data (KBr pellet): $\tilde{\nu}$ = 3074 (w), 2964 (w), 2074 (vs), 2048 (vs), 1600 (s), 1570 (m), 1470 (m), 1438 (s), 1334 (m), 1060 (s), 1014 (m), 776 (m), 754 (m), 680 (m) cm^{-1}. X-ray quality crystals of **2** were obtained by slow diffusion of a dilute methanolic solution of $(py)_2CO$ into a dilute aqueous solution of $Co(O_2CCH_3)_2 4H_2O$ and NaN_3. Complex **2** can also be isolated by employing $Co(O_2CCH_3)_2 4H_2O/(py)_2CO/NaN_3$ molar ratios of 1:2:2, 1:3:3, 1:2:4 and 1:4:4.

CAUTION: Azide salts are potentially explosive and should be handled in small quantities.

X-ray Structure Determinations: Crystals of **1** and **2** were mounted in air and in a capillary filled with drops of the mother liquor, respectively. Diffraction measurements were made on a Crystal Logic Dual Goniometer diffractometer using graphite-monochromated Mo-K_α radiation. Complete crystal data and parameters for data collection and refinement are listed in Table 3. Unit cell dimensions were determined and refined using the angular settings of 25 automatically centred reflections in the range $11 < 2\theta < 23°$.

Table 3. Crystal data and structure refinement for $[Mn_4(\mu_{1,1}\text{-}N_3)_2(N_3)_2\{(py)_2C(OH)O\}_2\{(py)_2C(OCH_3)O\}_2]$ (**1**) and $[Co_4(\mu_{1,1}\text{-}N_3)_2(N_3)_2\{(py)_2C(OH)O\}_2\{(py)_2C(OCH_3)\text{-}O\}_2]{\cdot}2H_2O$ (**2**)

Parameter	**1**	**2**
Empirical formula	$C_{46}H_{40}Mn_4N_{20}O_8$	$C_{46}H_{44}Co_4N_{20}O_{10}$
Mol. wt.	1220.72	1272.74
Colour and habit	Orange prisms	Pink prisms
Crystal size [mm]	0.10 × 0.20 × 0.30	0.15 × 0.35 × 0.55
Crystal system	Monoclinic	Triclinic
Space group	$P2_1/n$	$P\bar{1}$
a [Å]	13.391(4)	13.593(8)
b [Å]	12.503(4)	10.143(6)
c [Å]	16.007(6)	10.272(6)
α [°]	90.00	82.37(2)
β [°]	107.08(1)	73.83(2)
γ [°]	90.00	88.50(2)
V [Å^3]	2561.5(2)	1348.0(1)
Z	2	1
ρ [Mg m^{-3}]	1.583	1.568
T [°C]	25	25
λ(Mo-K_α) [Å]	0.71073	0.71073
μ [mm^{-1}]	1.037	1.284
F(000)	1240	648
$2\theta_{max}$ [°]	48.9	50.0
Index ranges [°]	$-15 \le h \le 14$	$-16 \le h \le 15$
	$0 \le k \le 14$	$-12 \le k \le 11$
	$0 \le l \le 18$	$-12 \le l \le 0$
No. of reflections collected	4369	5013
No. of indep. refls./R_{int}	4208/0.0506	4730/0.0148
Data with $I > 2\sigma(I)$	4208	4238
Parameters refined	432	433
$[\Delta/\sigma]_{max}$	0.014	0.034
GOF (on F^2)	1.023	1.093
$R1$[a]	0.0554	0.0363
$wR2$[b]	0.1433	0.1120
Residuals [e Å^{-3}]	0.564/-0.630	0.625/−0.447

[a] $R1 = \Sigma(|F_o| - |F_c|)/\Sigma(|F_o|)$. − [b] $wR2 = \{\Sigma[w[(F_o^2 - F_c^2)^2]/\Sigma[w(F_o^2)^2]\}^{1/2}$.

Intensity data were recorded using the θ-2θ scan method. Three standard reflections monitored every 97 reflections showed less than 3% variation and no decay. Lorentz, polarisation and Ψ-scan absorption (only for **2**) corrections were applied with the Crystal Logic software.

The structures were solved by direct methods using SHELXS-86[52] and refined by full-matrix least-squares techniques on F^2 with SHELXL-93.[53] All hydrogen atoms [except those of C(12) in **2** which were introduced at calculated positions as riding on their bonded atom] were located by difference maps and their positions refined isotropically. All non-hydrogen atoms of **1** and **2** were refined anisotropically, with the exception of the oxygen atoms of the solvent H_2O molecules in **2** which were refined isotropically with fixed occupation factors. Further details (excluding structure factors) for the structures reported in this paper have been deposited with the Cambridge Crystallographic Data Centre as supplementary publication nos. CCDC-147441 (**1**) and CCDC-147442 (**2**). Copies of the data can be obtained free of charge on application to CCDC, 12 Union Road, Cambridge CB2 1EZ [Fax: (internat.) +44-1223/336-033; E-mail: deposit@ccdc.cam.ac.uk].

Acknowledgments

This research was partially supported by CICYT (Grant PB96/0163), by the Research Committee of the University of Patras (K. CARATHEODORY Program No 1941 to S.P.P.), and the Greek Secretariat of Athletics, OPAP (to A. T.).

[1] D. Gatteschi, R. Sessoli, A. Cornia, *Chem. Commun.* **2000**, 725.
[2] J. Yoo, E. K. Brechin, A. Yamaguchi, M. Nakano, J. C. Huffman, A. L. Maniero, L. -C. Brunel, K. Awaga, H. Ishimoto, G. Christou, D. N. Hendrickson, *Inorg. Chem.* **2000**, *39*, 3615, and references cited therein.
[3] [3a] R. E. P. Winpenny, *Comments Inorg. Chem.* **1999**, *20*, 233. – [3b] J. M. Clemente-Juan, E. Coronado, *Coord. Chem. Rev.* **1999**, *193–195*, 361, and references cited therein.
[4] G. Aromi, J. -P. Claude, M. J. Knapp, J. C. Huffman, D. N. Hendrickson, G. Christou, *J. Am. Chem. Soc.* **1998**, *120*, 2977.
[5] E. Ruiz, J. Cano, S. Alvarez, P. Alemany, *J. Am. Chem. Soc.* **1998**, *120*, 11122.
[6] M. A. M. Abu-Youssef, A. Escuer, D. Gatteschi, M. A. S. Goher, F. A. Mautner, R. Vicente, *Inorg. Chem.* **1999**, *38*, 5716.
[7] M. A. M. Abu-Youssef, A. Escuer, M. A. S. Goher, F. A. Mautner, G. J. Reis, R. Vicente, *Angew. Chem. Int. Ed.* **2000**, *39*, 1624.
[8] M. A. M. Abu-Youssef, A. Escuer, M. A. S. Goher, F. A. Mautner, R. Vicente, *Eur. J. Inorg. Chem.* **1999**, 687.
[9] R. Cortés, M. Drillon, X. Solans, L. Lezama, T. Rojo, *Inorg. Chem.* **1997**, *36*, 677.
[10] R. Cortés, L. Lezama, J. L. Pizarro, M. I. Arriortua, T. Rojo, *Angew. Chem. Int. Ed. Engl.* **1996**, *35*, 1810.
[11] R. Cortés, L. Lezama, J. L. Pizarro, M. I. Arriortua, X. Solans, T. Rojo, *Angew. Chem. Int. Ed. Engl.* **1994**, *33*, 2488.
[12] R. Cortés, J. L. Pizarro, L. Lezama, M. I. Arriortua, T. Rojo, *Inorg. Chem.* **1994**, *33*, 2697.
[13] A. Escuer, R. Vicente, M. A. S. Goher, F. A. Mautner, *Inorg. Chem.* **1995**, *34*, 5707.
[14] A. Escuer, R. Vicente, M. A. S. Goher, F. A. Mautner, *Inorg. Chem.* **1996**, *35*, 6386.
[15] A. Escuer, R. Vicente, M. A. S. Goher, F. A. Mautner, *Inorg. Chem.* **1997**, *36*, 3440.
[16] A. Escuer, R. Vicente, M. A. S. Goher, F. A. Mautner, *J. Chem. Soc., Dalton Trans.* **1997**, 4431.
[17] A. Escuer, R. Vicente, M. A. S. Goher, F. A. Mautner, *Inorg. Chem.* **1998**, *37*, 782.
[18] M. A. S. Goher, N. A. Al-Salem, F. A. Mautner, *J. Coord. Chem.* **1998**, 119.
[19] M. A. S. Goher and F. A. Mautner, *Croat. Chim. Acta* **1990**, *63*, 559.
[20] J. L. Manson, A. M. Arif, J. S. Miller, *Chem. Commun.* **1999**, 1479.
[21] F. A. Mautner, R. Cortés, L. Lezama, T. Rojo, *Angew. Chem. Int. Ed. Engl.* **1996**, *35*, 78.
[22] F. A. Mautner, S. Hanna, R. Cortés, L. Lezama, M. G. Barandika, T. Rojo, *Inorg. Chem.* **1999**, *38*, 4647.
[23] H. Y. Shen, D. Z. Liao, Z.-H. Jiang, S.-P. Yan, B.-W. Sun, G.-L. Wang, X.-K. Yao, H.-G. Wang., *Chem. Lett.* **1998**, 469.
[24] Z. Shen, J.-L. Zuo, Z. Yu, Y. Zhang, J.-F. Bai, C.-M. Che, H.-K. Fun, J.-J. Vittal, X. -Z. You, *J. Chem. Soc., Dalton Trans.* **1999**, 3393.
[25] M. A. Youssef, A. Escuer, M. A. S. Goher, F. A. Mautner, R. Vicente, *J. Chem. Soc., Dalton Trans.* **2000**, 413.
[26] Z. E. Serna, L Lezama, M. K. Urtiaga, M. I. Arriortua, M. G. Barandika, R. Cortés, T. Rojo, *Angew. Chem. Int. Ed.* **2000**, *39*, 344.
[27] Z. E. Serna, M. G. Barandika, R. Cortés, M. K. Urtiaga, G. A. Barberis, T. Rojo, *J. Chem. Soc., Dalton Trans.* **2000**, 29.
[28] A. C. Deveson, S. L. Heath, C. J. Harding, A. K. Powell, *J. Chem. Soc., Dalton Trans.* **1996**, 3173.
[29] J. Manzur, A. M. García, M. T. Garland, V. Acuña, O. Gonzalez, O. Peña, A. M. Atria, E. Spodine, *Polyhedron* **1996**, *105*, 821.
[30] V. Tangoulis, C. P. Raptopoulou, S. Paschalidou, A. E. Tsohos, E. G. Bakalbassis, A. Terzis, S. P. Perlepes, *Inorg. Chem.* **1997**, *36*, 5270.
[31] S. R. Breeze,S. Wang, J. E. Greedan, N. P. Raju, *Inorg. Chem.* **1996**, *35*, 6944.
[32] A. Tsohos, S. Dionyssopoulou, A. Terzis, E. G. Bakalbassis, S. P. Perlepes, *Angew. Chem. Int. Ed.* **1999**, *38*, 983.
[33] M.-L. Tong, H. K. Lee, S.-L. Zheng, X. -M. Chen, *Chem. Lett.* **1999**, 1087.
[34] V. Tangoulis, C. P. Raptopoulou, S. Paschalidou, E. G. Bakalbassis, S. P. Perlepes, A. Terzis, *Angew. Chem. Int. Ed. Engl.* **1997**, *36*, 1083.
[35] V. Tangoulis, S. Paschalidou, E. G. Bakalbassis, S. P. Perlepes, C. P. Raptopoulou, A. Terzis, *Chem. Commun.* **1996**, 1297.
[36] V. Tangoulis, C. P. Raptopoulou, A. Terzis, S. Paschalidou, S. P. Perlepes, E. G. Bakalbassis, *Inorg. Chem.* **1997**, *36*, 3996.
[37] M. G. B. Drew, F. S. Esho, A. Lavery, S. M. Nelson, *J. Chem. Soc., Dalton Trans.* **1984**, 545.
[38] A. Bencini, C. A. Ghilardi, S. Midollini, A. Orlandini, *Inorg. Chem.* **1989**, *28*, 1958.
[39] G. De Munno, T. Poerio, G. Viau, M. Julve, F. Lloret, Y. Journaux, E. Riviere, *Chem. Commun.* **1996**, 2587.
[40] M. G. B. Drew, C. J. Harding, J. Nelson, *Inorg. Chim. Acta* **1996**, *246*, 73.
[41] A. Escuer, C. J. Harding, Y. Dussart, J. Nelson, V. McKee, R. Vicente, *J. Chem. Soc., Dalton Trans.* **1999**, 223.
[42] G. Viau, M. G. Lombardi, G. De Munno, M. Julve, F. Lloret, J. Faus, A. Caneschi, J. M. Clemente-Juan, *Chem. Commun.* **1997**, 1195.
[43] F. Meyer, K. Heinze, B. Nuber, L. Zsolnai, *J. Chem. Soc., Dalton Trans.* **1998**, 207.
[44] M. A. S. Goher, F. Mautner, *Polyhedron* **1999**, *18*, 2339.
[45] E. W. Constable, *Metals and Ligand Reactivity*, 2nd ed., VCH, Weinheim, Germany, **1996**, pp. 46–48, 57–59.
[46] C. K. Johnson, ORTEP II, Report ORNL-5138, Oak Ridge National Laboratory, Oak Ridge, TN, **1976**.

[47] D. Gatteschi, L. Pardi, *Gazz. Chim. Ital.* **1993**, *123*, 231.
[48] E. Ruiz, S. Alvarez, P. Alemany, *Chem. Commun.* **1998**, 2767.
[49] A. Abragam, B. Bleaney, in *Electron Paramagnetic Resonance of Transition Ions*, Oxford University Press, New York, **1986**, pp. 209−216.
[50] S. L. Dexheimer, J. W. Gohdes, M. K. Chan, K. S. Hagen, W. H. Armstrong, M. P. Klein, *J. Am. Chem. Soc.* **1989**, *111*, 8923.
[51] K. L. Kostka, B. G. Fox, M. P. Hendrich, T. J. Collins, C. E. F. Rickard, L. J. Wright, E. Münch, *J. Am. Chem. Soc.* **1993**, *115*, 6746.
[52] G. M. Sheldrick, *SHELXS-86*, *Program for the Solution of Crystal Structures*, University of Göttingen, Germany, **1986.**
[53] G. M. Sheldrick, *SHELXL-93*, *Program for the Refinement of Crystal Structures*, University of Göttingen, Germany, **1993.**

Received October 9, 2000
[I00378]